RESEARCH | SYNTHETIC YEAST GENOME

RESEARCH ARTICLE SUMMARY

SYNTHETIC BIOLOGY

Synthesis, debugging, and effects of synthetic chromosome consolidation: synVI and beyond

Leslie A. Mitchell, Ann Wang, Giovanni Stracquadanio, Zheng Kuang, Xuya Wang, Kun Yang, Sarah Richardson, J. Andrew Martin, Yu Zhao, Roy Walker, Yisha Luo, Hongjiu Dai, Kang Dong, Zuojian Tang, Yanling Yang, Yizhi Cai, Adriana Heguy, Beatrix Ueberheide, David Fenyö, Junbiao Dai, Joel S. Bader, Jef D. Boeke*

INTRODUCTION: Total synthesis of designer chromosomes and genomes is a new paradigm for the study of genetics and biological systems. The Sc2.0 project is building a designer yeast genome from scratch to test and extend the limits of our biological knowledge. Here we describe the design, rapid assembly, and characterization of synthetic chromosome VI (synVI). Further, we investigate the phenotypic, transcriptomic, and

some consolidation to uncover possible synthetic genetic interactions and/or perturbations of native cellular networks as the number of designer changes increases is the next major step for the Sc2.0 project.

RESULTS: SynVI was rapidly assembled using nine sequential steps of SwAP-In (switching auxotrophies progressively by integration), yielding a ~240-kb synthetic chromosome designed to
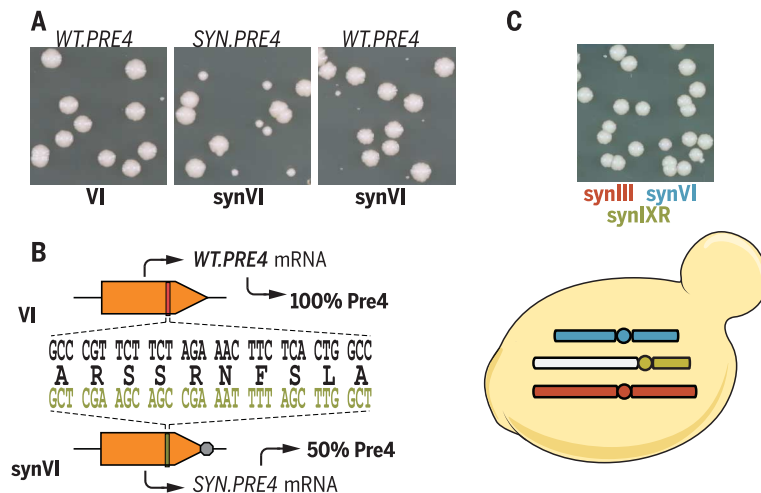
Debugging synVI and characterization of poly-synthetic yeast cells. (**A**) The second Sc2.0 chromosome to be constructed, synVI, encodes a "bug" that causes a variable colony size, dubbed a "glycerol-negative growth-suppression defect." (**B**) Synonymous changes in the essential *PRE4* ORF lead to a reduced protein level, which underlies the growth defect. (**C**) The poly-synthetic strain synIII synVI synIXR directs growth of yeast cells to near WT fitness levels.

proteomic consequences associated with consolidation of three synthetic chromosomes—synVI, synIII, and synIXR—into a single poly-synthetic strain.

RATIONALE: A host of Sc2.0 chromosomes, including synVI, have now been constructed in discrete strains. With debugging steps, where the number of bugs scales with chromosome length, all individual synthetic chromosomes have been shown to power yeast cells to near wild-type (WT) fitness. Testing the effects of Sc2.0 chromo-

Sc2.0 specifications. We observed partial silencing of the left- and rightmost genes on synVI, each newly positioned subtelomerically relative to their locations on native VI. This result suggests that consensus core X elements of Sc2.0 universal telomere caps are insufficient to fully buffer telomere position effects. The synVI strain displayed a growth defect characterized by an increased frequency of glycerol-negative colonies. The defect mapped to a synVI design feature in the essential *PRE4* gene (*YFR050C*), encoding the β7 subunit of the 20S proteasome. Recod-

ing 10 codons near the 3′ end of the *PRE4* open reading frame (ORF) caused a ~twofold reduction in Pre4 protein level without affecting RNA abundance. Reverting the codons to the WT sequence corrected both the Pre4 protein level and the phenotype. We hypothesize that the formation of a stem loop involving recoded codons underlies reduced Pre4 protein level.

ON OUR WEBSITE

Read the full article at http://dx.doi.org/10.1126/science.aaf4831

Sc2.0 chromosomes (synI to synXVI) are constructed individually in discrete strains and consolidated into poly-synthetic (poly-syn) strains by "endoreduplication intercross." Consolidation of synVI with synthetic chromosomes III (synIII) and IXR (synIXR) yields a triple-synthetic (triple-syn) strain that is ~6% synthetic overall—with almost 70 kb deleted, including 20 tRNAs, and more than 12 kb recoded. Genome sequencing of double-synthetic (synIII synVI, synIII synIXR, synVI synIXR) and triple-syn (synIII synVI synIXR) cells indicates that suppressor mutations are not required to enable coexistence of Sc2.0 chromosomes. Phenotypic analysis revealed a slightly slower growth rate for the triple-syn strain only; the combined effect of tRNA deletions on different chromosomes might underlie this result. Transcriptome and proteome analyses indicate that cellular networks are largely unperturbed by the existence of multiple synthetic chromosomes in a single cell. However, a second bug on synVI was discovered through proteomic analysis and is associated with alteration of the *HIS2* transcription start as a consequence of tRNA deletion and loxPsym site insertion. Despite extensive genetic alterations across 6% of the genome, no major global changes were detected in the poly-syn strain "omics" analyses.

CONCLUSION: Analyses of phenotypes, transcriptomics, and proteomics of synVI and poly-syn strains reveal, in general, WT cell properties and the existence of rare bugs resulting from genome editing. Deletion of subtelomeres can lead to gene silencing, recoding deep within an ORF can yield a translational defect, and deletion of elements such as tRNA genes can lead to a complex transcriptional output. These results underscore the complementarity of transcriptomics and proteomics to identify bugs, the consequences of designer changes in Sc2.0 chromosomes. The consolidation of Sc2.0 designer chromosomes into a single strain appears to be exceptionally well tolerated by yeast. A predictable exception to this is the deletion of tRNAs, which will be restored on a separate neochromosome to avoid synthetic lethal genetic interactions between deleted tRNA genes as additional synthetic chromosomes are introduced. ∎

The list of author affiliations is available in the full article online.
*Corresponding author. Email: jef.boeke@nyumc.org
Cite this article as L. A. Mitchell *et al.*, *Science* **355**, eaaf4831 (2017). DOI: 10.1126/science.aaf4831

Downloaded from http://science.sciencemag.org/ on March 10, 2017

Mitchell *et al.*, *Science* **355**, 1045 (2017)   10 March 2017

1 of 1

RESEARCH ARTICLE

SYNTHETIC BIOLOGY

Synthesis, debugging, and effects of synthetic chromosome consolidation: synVI and beyond

Leslie A. Mitchell,[1,2] Ann Wang,[3,4] Giovanni Stracquadanio,[3,5,6] Zheng Kuang,[1,2]
Xuya Wang,[1,2] Kun Yang,[3,5] Sarah Richardson,[3,5] J. Andrew Martin,[1,2] Yu Zhao,[1,2]
Roy Walker,[7] Yisha Luo,[7] Hongjiu Dai,[8] Kang Dong,[8] Zuojian Tang,[1,2] Yanling Yang,[9]
Yizhi Cai,[7] Adriana Heguy,[10] Beatrix Ueberheide,[1,9] David Fenyö,[1,2] Junbiao Dai,[4]
Joel S. Bader,[3,4] Jef D. Boeke[1,2]*

We describe design, rapid assembly, and characterization of synthetic yeast Sc2.0 chromosome VI (synVI). A mitochondrial defect in the synVI strain mapped to synonymous coding changes within *PRE4* (*YFR050C*), encoding an essential proteasome subunit; Sc2.0 coding changes reduced Pre4 protein accumulation by half. Completing Sc2.0 specifies consolidation of 16 synthetic chromosomes into a single strain. We investigated phenotypic, transcriptional, and proteomewide consequences of Sc2.0 chromosome consolidation in poly-synthetic strains. Another "bug" was discovered through proteomic analysis, associated with alteration of the *HIS2* transcription start due to transfer RNA deletion and loxPsym site insertion. Despite extensive genetic alterations across 6% of the genome, no major global changes were detected in the poly-synthetic strain "omics" analyses. This work sets the stage for completion of a designer, synthetic eukaryotic genome.

Total synthesis of designer chromosomes and genomes is a new paradigm for the study of genetics and biological systems. The Sc2.0 project is building a designer yeast genome from scratch to test and extend the limits of our biological knowledge.

SynVI—Design, assembly, and debugging

Here we report the construction of the second full-length Sc2.0 chromosome, synVI, designed to Sc2.0 specifications using the genome-editing suite BioStudio (Fig. 1A and fig. S1) (*1*, *2*). Although all

[1]Department of Biochemistry and Molecular Pharmacology, New York University Langone School of Medicine, New York, NY 10016, USA. [2]Institute for Systems Genetics, New York University Langone School of Medicine, New York, NY 10016, USA. [3]High Throughput Biology Center, Johns Hopkins University School of Medicine, Baltimore, MD 21205, USA. [4]Key Laboratory for Industrial Biocatalysis (Ministry of Education), Key Laboratory of Bioinformatics (Ministry of Education), Center for Synthetic and Systems Biology, School of Life Sciences, Tsinghua University, Beijing 100084, China. [5]Department of Biomedical Engineering and Institute of Genetic Medicine, Whiting School of Engineering, Johns Hopkins University, Baltimore, MD 21218, USA. [6]School of Computer Science and Electronic Engineering, University of Essex, Wivenhoe Park, Colchester CO4 3SQ, UK. [7]Center for Synthetic and Systems Biology, School of Biological Sciences, University of Edinburgh, Edinburgh EH9 3JL, UK. [8]GenScript, Piscataway, NJ 08854, USA. [9]Proteomics Resource Center, Office of Collaborative Science, New York University Langone School of Medicine, New York, NY 10016, USA. [10]Genome Technology Center, New York University Langone School of Medicine, New York, NY 10016, USA.
*Corresponding author. Email: jef.boeke@nyumc.org

five spliceosomal introns in native chromosome VI genes were deleted, a single specialized non-spliceosomal intron, encoded by *HAC1* (*YFL031W*), was retained because of its critical role in regulation of the unfolded protein response (*3*, *4*). Retaining this intron remains consistent with an overall Sc2.0 project goal to remove all spliceosomal introns and eventually test whether the spliceosome has biological functions beyond removing introns from pre-mRNAs. The final synVI designed chromosome is 242,745 base pairs (bp) in length, 11.3% shorter than native VI.

SynVI was efficiently assembled using SwAP-In (switching auxotrophies progressively by integration) (*1*, *2*), enabled by segmentation of the designed chromosome into 9 megachunks (each of 30 to 40 kb) and 26 chunks (~10-kb each) (Fig. 1A). The production of 10-kb chunks was performed using standard gene-assembly methods, and nearly all chunks were successfully built as full-length, sequence-verified constructs. In nine sequential steps, we incorporated more than 240 kb of synthetic DNA into a haploid yeast strain to build synVI (Fig. 1B). At each integration step, clones that exclusively produced synthetic polymerase chain reaction tag (PCRTag) amplicons, used as watermarks for the synthetic sequence (*2*), were identified (fig. S2). DNA sequencing of the synVI genome revealed 10 point mutations on synVI compared with the designed sequence. All point mutations were in open reading frames, and five yielded nonsynonymous mutations (table S1). Only 2 of the 10 point mutations recovered

on synVI were de novo as a result of incorporation (*5*), corresponding to a mutation frequency of ~1 × 10⁻⁵, similar to that observed for synIII (*6*). Two nonsynonymous mutations affected the essential *MOB2* gene (*YFL034C-B*) and conferred a notable fitness defect (fig. S3); their correction to the designed sequence substantially improved growth (fig. S4) (*5*).

RNA sequence (RNA-seq) profiling of synVI strains [yLM175 (yeast_chr06_9_01) and yLM953 (yeast_chr06_9_03)] revealed only a small number of significant changes in gene expression relative to the wild type (Fig. 1C and fig. S5). The two significantly down-regulated genes on synVI each lie adjacent to a terminal universal telomere cap (UTC) (*6*): *YFL055W* encoding Agp3, a low-affinity amino acid permease (*7*), and *YFR055W* encoding Irc7, a beta-lyase involved in thiol production (*8*). To test for gene silencing by telomere position effect (TPE) due to deleting native subtelomeres (Fig. 1C, inset), we generated circularized derivatives of native VI and synVI (Fig. 1B) (*5*). Expression of *YFL055W* and *YFR055W* from ring synVI was similar to levels observed in the native linear VI strain (Fig. 1D). Native VI subtelomeres encode core X elements, and the left subtelomere contains a Y′ element. Although the core X sequence clearly has some insulator-like function (*9*), our data indicate that consensus core X elements of the UTC are insufficient to fully insulate telomere-proximal promoters from TPE and suggests that one function of long subtelomeric regions is to fully buffer the transcriptome against silencing.

After correcting nonsynonymous mutations in *MOB2*, the synVI strain [yLM402 (yeast_chr06_9_02)] still had a noticeable growth defect or "bug" characterized by variable colony size, with roughly half of all colonies growing to a smaller overall size. The small colonies were respiratory-deficient, as they could not grow on medium with glycerol as the sole carbon source. Analysis of the mitochondrial DNA (mtDNA) of the glycerol-negative synVI colonies revealed that segments of the *15S rRNA*, *ATP6*, and *COX2* genes were lost at high frequency (fig. S6). Glycerol-negative synVI colonies were surprisingly large relative to glycerol-negative derivatives of wild-type (WT) cells. This "glycerol-negative growth-suppression defect" is best visualized by comparing the colony size of WT and synVI cells pretreated in ethidium bromide, which converts cells to ρ^0 by inducing the loss of mtDNA (Fig. 1E). The defect did not depend on nonsynonymous synVI mutations (table S1 and fig. S7). We also evaluated the fitness of the synVI strain by plating serial dilutions on a diverse panel of media and growth conditions (*6*) and found no condition that substantially affected growth (fig. S8).

We mapped the defect to the gene *PRE4* (*YFR050C*) using a meiotic recombination strategy (Fig. 1, F and G, and figs. S9 to S13) (*5*). *PRE4* encodes the essential β7 subunit of the 20*S* proteasome (*10*). The Pre4 C terminus plays a structural role in 20*S* proteasome assembly (*11*) while the N-terminal eight amino acids are processed (*12*) upon assembly (*13*). To test whether a reduced *PRE4* copy

number might underlie the glycerol-negative growth-suppression defect, we made diploids heterozygous for *PRE4* in VI/VI or synVI/synVI strains. The VI/VI *pre4Δ/PRE4* strain displayed a phenotype very similar to that of the *PRE4/PRE4* synVI/synVI strain (Fig. 2A). The designer features encoded by the *SYN.PRE4* allele include a TAG/TAA stop-codon swap and a PCRTag pair with recoded sequences encompassing 10 codons each (Fig. 2, B and C). Installing the *WT.PRE4* allele into synVI or the *SYN.PRE4* allele into native VI rescued or phenocopied the glycerol-negative growth-suppression defect, respectively (Fig. 2D). The defect was further tracked to the synthetic PCRTag closer to the *PRE4* 3′ end (Fig. 2D). We also introduced individual WT codons into an otherwise synthetic *PRE4* allele in the synVI background and found that no single WT codon could rescue the glycerol-negative growth-suppression defect entirely (fig. S14). However, WT codons at positions S4, R5, and N6 showed partial rescue, and replacing four consecutive rare codons (R2, S3, S4, R5) with the WT versions (*WT.RSSR*) in synthetic *PRE4* on synVI rescued the defect (fig. S14). Conversely, introducing the four rare codons (*SYN.RSSR*) into WT *PRE4* on native VI was insufficient to phenocopy the defect (fig. S14).

Genetic analyses suggested that *PRE4* was underexpressed in synVI. Given that the *PRE4* transcript level was normal (Fig. 1C and fig. S5) (*5*), we examined Pre4 protein accumulation. Haploid strains expressing either synthetic (*SYN.PRE4*) or WT (*WT.PRE4*) alleles with N-terminal HA tags were constructed; each was integrated into the WT (VI) or synthetic (synVI) *PRE4* chromosomal locus. Although the Pre4 N terminus is cleaved (*12*), we tagged this end rather than the C terminus to capture potential translational frameshifts predicted to result in changes in protein length. We found that strains encoding *SYN.PRE4* expressed about half as much Pre4 protein product as *WT.PRE4*, irrespective of chromosomal context (native VI or synVI). No protein products of unexpected molecular weight were observed (Fig. 2E). PCRTag recoding, leading to protein-related defects, could result from a ribosomal stall, underpinned by generation or destruction of RNA modification sites, formation of previously unidentified mRNA secondary structure, or an imbalance between tRNA supply and demand. Any of these factors could reduce protein accumulation by reducing translational output or causing misfolding coupled to protein degradation. In the synVI strain, 10 tRNA genes were deleted and more than 9000 bp were recoded (table S2). However, WT cells expressing the *WT-SYN.PRE4* allele in the native VI background phenocopied the glycerol-negative growth-suppression defect, which suggests a mechanism independent of tRNA supply and demand. Consistent with this, episomal expression of the 10 tRNAs deleted from synVI had no effect on Pre4 protein level (fig. S14).

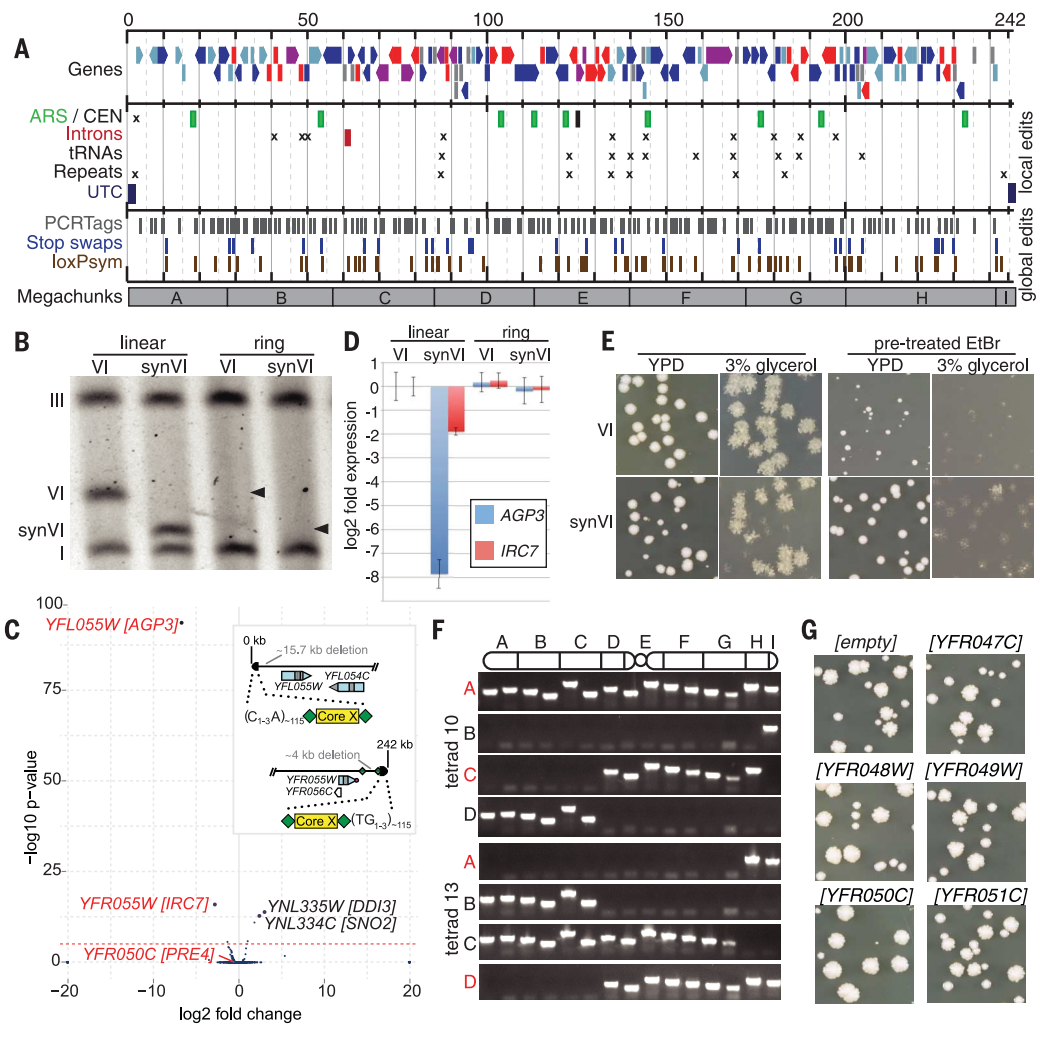**Fig. 1. SynVI design, assembly, and bug mapping.** (**A**) The ~242-kb synthetic chromosome VI (synVI) encodes all designer features of Sc2.0 chromosomes (*1*, *2*, *6*). Deleted elements are denoted with the letter "x." SynVI is segmented into nine megachunks (A to I) for SwAP-In (switching auxotrophies progressively by integration). Gene order and orientation are indicated (red, essential; purple, required for fast growth; dark blue, nonessential with function characterized; light blue, nonessential with uncharacterized function; gray, dubious). UTC, universal telomere cap; ARS, autonomously replicating sequence; CEN, centromere. (**B**) SynVI (~242 kb) (yLM402) migrates faster than native VI (~270 kb) (BY4741) by pulsed-field gel electrophoresis. Circular derivatives of native VI (yLM717) and synVI (yLM728) do not penetrate the gel (black arrowheads). (**C**) RNA-seq data of synVI (yLM953) represented as a volcano plot. Genes on synVI are shown in red. (Inset) Schematic of synVI telomeres along with right- and leftmost genes. Sc2.0 UTCs encode consensus core X elements flanked by loxPsym sites (green diamonds) with flanking yeast telomere repeat sequence [(C$_{1-3}$A)$_{~115}$; (TG$_{1-3}$)$_{~115}$]. (**D**) Relative expression of *AGP3* and *IRC7* from strains carrying native VI or synVI in linear (BY4741, yLM402) or ring structures (yLM718, yLM728). Error bars indicate SD. (**E**) The synVI strain (yLM402) produces glycerol-negative colonies that grow faster on yeast extract peptone dextrose (YPD) medium than native VI. Spontaneously generated glycerol-negative colonies (left) compared with ρ^0 cells generated by pretreatment in ethidium bromide (EtBr) (right). (**F**) Meiotic PCRTag mapping of two full tetrads (10 and 13, A to D) (backcross of synVI strain yLM402 to WT strain BY4742), with 15 synthetic PCRTags spanning synVI from left to right. Native VI is inferred by the absence of amplicons. Red lettering denotes spores with growth defects, as shown by single-colony growth. Also see figs. S9 and S10. (**G**) An extra copy of synthetic *YFR050C* rescues the synVI growth defect (yLM707, yLM875-yLM878).

In silico mRNA secondary structure prediction of sequence spanning the synthetic PCRTag indicates potential formation of a stem loop mediated by recoded bases (S4 and R5 codons pairing with L9 and A10) (Fig. 2F). Involvement of S4 and R5 in a stem loop is consistent with our genetic data (fig. S14) and, taken together with ruling out tRNA supply and demand, implicates secondary structure of the *SYN.PRE4* mRNA transcript as mechanistically underlying reduced Pre4 protein level. The connection between Pre4 level and the glycerol-negative growth-suppression defect remains to be explored.

Effects of consolidation of synthetic chromosomes

The Sc2.0 chromosomes (synI to synXVI) are being constructed individually in discrete strains (*1*, *2*, *6*). Using "endoreduplication intercross," poly-synthetic (poly-syn) chromosome strains encoding two (synIII synVI; synIII synIXR; synVI synIII) and three synthetic chromosomes (synIII synVI synIXR) were constructed (*1*). The triple-synthetic strain (triple-syn) is ~6% synthetic overall, with almost 70 kb deleted (including 20 tRNAs) and more

than 12 kb recoded (table S2). Genome sequencing of the four poly-syn strains uncovered only a small number of point mutations relative to design (table S3), all of which were common to all sequenced strains, indicating that they existed before endoreduplication intercrossing. This result suggests that new suppressor mutations need not arise to enable coexistence of multiple synthetic chromosomes.

To further evaluate the effects of consolidating synthetic chromosomes, we undertook phenotypic, transcriptomic, and proteomic profiling of poly-syn strains. We compared the growth of poly-syn strains to that of WT strains and observed a ~15% increase in doubling time of the triple-syn strain in a multiwell-plate liquid culture growth assay (Fig. 3A). However, overall colony size and morphology on both yeast extract peptone dextrose (YPD) and 3% glycerol plates at 30° and 37°C were comparable after 7 days (Fig. 3B). In contrast, colony size on synthetic complete medium was slightly smaller for triple-syn cells than for the wild type (Fig. 3B). One possible cause underlying reduced growth of the synIII synVI synIXR strain is the deletion of 20 tRNAs (table S2). Importantly, as increasing numbers of syn-

thetic chromosomes are consolidated, the deleted tRNAs will be restored on a separate neochromosome. Doubling time, colony size, and morphology were generally indistinguishable from the wild type for all double-synthetic (double-syn) strains on all media types and conditions tested (Fig. 3A and fig. S15).

RNA sequencing of poly-syn strains revealed only a small number of significant transcriptome changes in the poly-syn strains (Fig. 3C and fig. S16) (*5*). Surprisingly, in the triple-syn strain, expression of the four genes encoded by the native 2-micron plasmid (*FLP1*, *REP1*, *REP2*, *RAF1*) (*14*) was significantly reduced (Fig. 3C). From genome sequence data, the depth of reads mapping to the 2-micron plasmid was virtually nonexistent, suggesting that the 2-micron plasmid had nearly been lost from the triple-syn strain at the time of sequencing. Curiously, outright loss of the 2-micron plasmid was not observed in any of the double-syn chromosome strains, although it was absent in an early version of the synX strain (*15*). Endoreduplication backcross of synX led to recovery of the 2-micron plasmid, which suggests that its loss is not a function of the synthetic chromosomes.
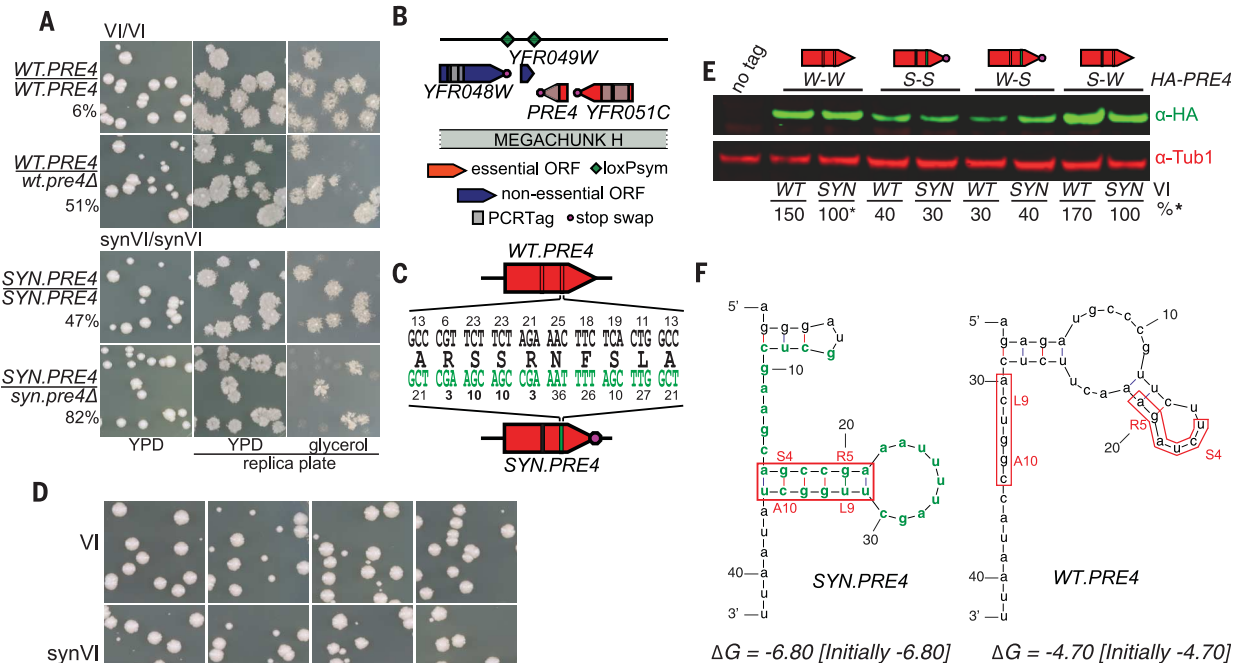
Fig. 2. *PRE4* PCRTag recoding underlies *synVI* glycerol-negative growth-suppression defect. (**A**) *PRE4* haploinsufficiency. Deleting one copy of *PRE4* (*WT/WT WT.PRE4/wt.pre4Δ*; yLM770) in the wild-type (WT) diploid (VI/VI; BY4743) phenocopies the glycerol-negative growth-suppression defect observed in the synVI diploid (synVI/synVI; yLM544) and synVI *SYN.PRE4* heterozygous diploids (synVI/synVI *PRE4/pre4Δ*; yLM772). Glycerol-negative colony frequency as percentage of total colonies is indicated. (**B**) Synthetic *YFR050C/ PRE4* locus. ORF, open reading frame. (**C**) *PRE4* WT and synthetic (SYN) PCRTag sequences are synonymous. Codon usage is indicated as frequency per thousand codons. (**D**) Installing the 3′ synthetic PCRTag (green bar) provokes the defect in WT cells (VI) and rescues the defect in synVI cells. PCRTags in the

synthetic *PRE4* allele (*SYN.PRE4*). The 5′ PCRTag (black bar) has no impact. (Strains, top row: BY4741, yLM849, yLM853, yLM851; bottom row: yLM949, yLM402, yLM957, yLM953.) (**E**) Pre4 protein level. N-terminally HA-tagged Pre4, expressed from the *PRE4* locus on synVI or native VI as a synthetic or WT allele. Protein level is expressed as a percentage of the wild type. (Strains, from left to right: BY4741, yLM883, yLM882, yLM867, yLM866, yLM1212, yLM1214, yLM1216, yLM1218.) (**F**) mFold secondary structure predictions for *SYN.PRE4* and *WT. PRE4* alleles. Predictions were generated using the 20 bases of the 3′ *PRE4* PCRTag plus 6 flanking bases using the mFold Web server (*31*). 3′ *PRE4* PCRTag codons S4, R5, A10, and L9 are indicated in red boxes for the synthetic (left, *SYN.PRE4*) and WT (right, *WT.PRE4*) alleles. ΔG, change in Gibbs free energy.

Rather, it is likely that the loss of the 2-micron plasmid is a consequence of multiple rounds of genetic manipulation and single-colony purification.

PRE4 recoding reduced protein expression. To test for more widespread proteome changes in the triple-syn strain, mediated by recoding events and/or tRNA supply and demand, we used tandem mass tag labeling to quantitatively evaluate the triple-syn proteome relative to the wild type. The *SYN-WT.PRE4* allele was encoded in the triple-syn strain, so we did not expect altered levels of Pre4 protein. Of 3122 proteins whose relative abundance was determined, only 11 displayed significantly altered levels in the triple-syn strain (Fig. 3D and table S4). We directly tested six of these proteins by immunoblot analysis and confirmed altered expression only for His2, encoded by synVI (Fig. 3E and fig. S17). We found that His2 protein level depended on presence of an upstream tRNA gene [*tA(AGC)F*] and that its replacement with a loxPsym site
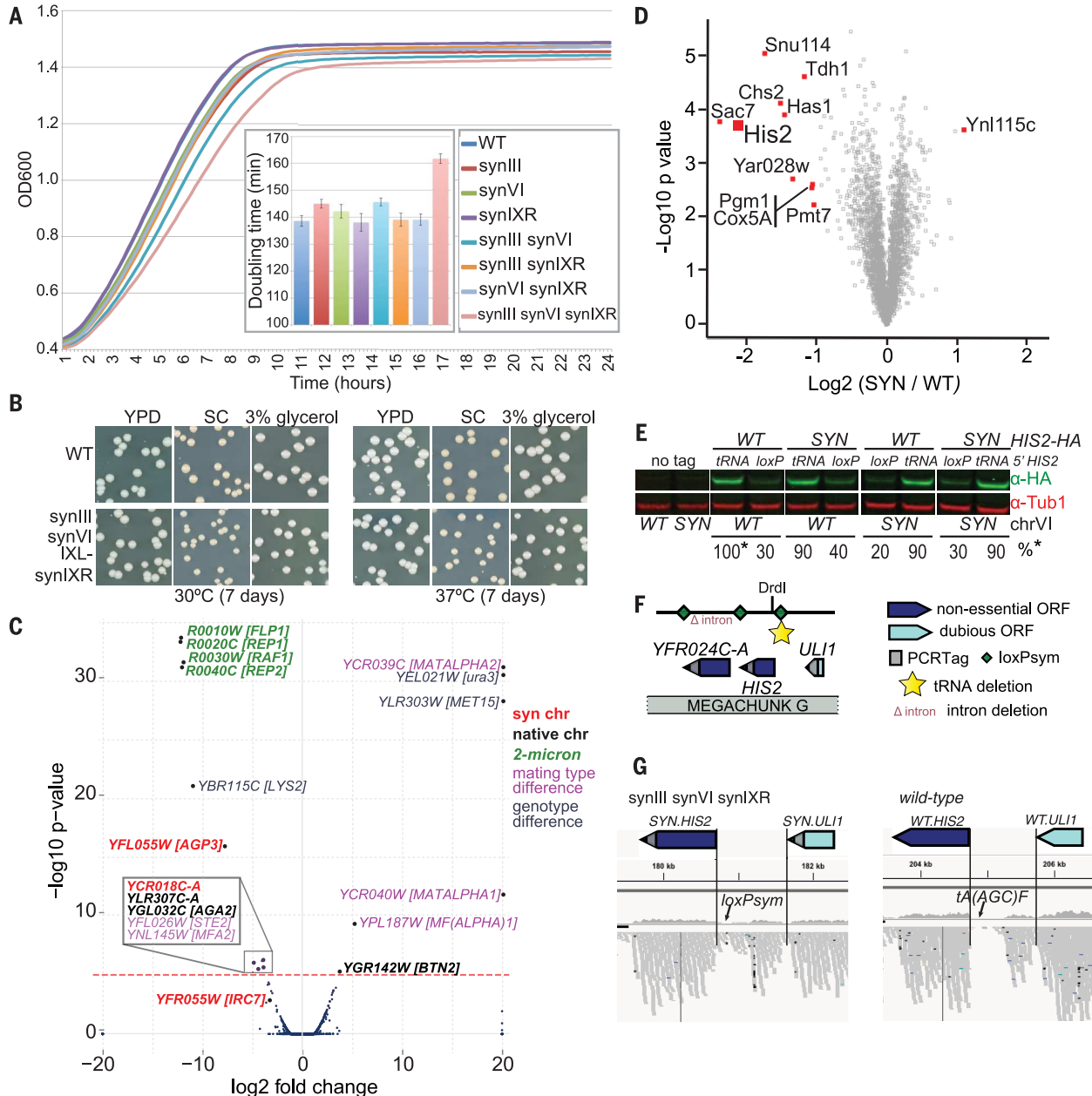
Fig. 3. Poly-synthetic strain characterization. (**A**) Growth curve and doubling time of synthetic strains (30°C, YPD, 24 hours). (Strains: BY4741, yLM422, yLM953, yLM461, yLM890, yLM758, yLM892, yLM896.) Error bars indicate SD. OD, optical density. (**B**) Colony size and morphology of the triple-synthetic (triple-syn) strain (yLM896) compared with the wild type (BY4742). (**C**) RNA-seq data of the triple-syn strain (yLM896) represented as a volcano plot. Genes are categorized according to color as indicated. The triple-syn strain (*MATα MET15, lys2Δ0, ura3*) transcriptome was determined relative to that of a WT strain (BY4741; *MATa, met15Δ, LYS2, ura3Δ0*). Genotypic differences underlie most differentially expressed genes. (**D**) Whole-proteome analysis of triple-syn cells (SYN) (yLM896) compared with WT cells (BY4742). Proteins with significantly changed expression are shown in red and named. (**E**) Immunoblot evaluating expression of tagged SYN or WT *HIS2* (*HIS2-HA*) from either the native VI (WT) or synVI (SYN) chromosome. Inserted upstream of *HIS2* is either the native tRNA gene [*tA(AGC)F*] or a loxPsym site. Intervening lanes are cropped. (Strains, from left to right: BY4741, yLM953, yLM1198 to yLM1205.) (**F**) The synthetic *HIS2* locus. (**G**) RNA-seq reads mapping to the *SYN.HIS2* and *WT.HIS2* alleles from the triple-syn and WT strains. The position of the tRNA gene [*tA(AGC)F*] in native VI and the loxPsym site replacing it in the synVI chromosome are indicated.

decreased cellular His2 levels (Fig. 3, E and F). In the triple-syn RNA-seq data set, we discovered a set of reads mapping upstream of the *HIS2* start site that were absent from the wild type (Fig. 3G). Replacement of the tRNA with a loxPsym site may create a cryptic start site, such that not all mRNA yields His2 translation product and/or that transcription from the upstream region might interfere with expression from the native His2 promoter (Fig. 3G). This result underscores the importance of proteomic analysis as a complementary tool to RNA-seq to identify consequences of designer changes in Sc2.0 chromosomes. In total, quantitative proteomic analysis allowed us to evaluate relative expression level of ~50% of proteins encoded by chromosomes synIII, synVI, and synIXR. The paucity of changes indicates minimal impact on the proteome from designer changes to the genome sequence.

Conclusions

Phenotypic, transcriptomic, and proteomic analysis of the synVI and poly-syn strains reveals, in general, a WT set of properties, with at least three unexpected "bugs" resulting from genome editing. Deletion of subtelomeres led to synVI terminal gene silencing, recoding deep within *PRE4* resulted in a translational defect, and deletion of an upstream tRNA gene caused a translational phenotype associated with activation of a cryptic start site and/or promoter interference. Consolidation of Sc2.0 designer chromosomes into a single strain appears to be exceptionally well tolerated by yeast, despite the large number of designer changes. As additional synthetic chromosomes are introduced, deleted tRNA genes will be restored on a separate "neochromosome" to avoid synthetic genetic interactions between tRNA gene deletions.

Materials and methods
Chunk synthesis and in vitro megachunk assembly

With a few exceptions (chunks A1 and B3, see below) synthetic DNA constructs were delivered as subcloned and sequence-verified ~10 kb chunks. All chunk constructs were transformed into *E. coli* and grown at either 25°C (chunk C1) or 30°C (all other constructs). Top10 cells were used to propagate all chunk constructs except F1 and F3, which were transformed in CopyCutter EPI-400 cells (Epicenter, C400CH10) to maintain low copy number prior to the addition of Induction Solution (Epicentre, CIS40025) to the liquid growth medium as per the manufacturer's instructions. Constructs were isolated from saturated bacterial cultures by standard alkaline lysis followed by isopropanol precipitation. ~5 μg was digested with the appropriate restriction enzymes and the synthetic DNA fragments gel-purified using the Zymoclean Large Fragment DNA Recovery Kit (Zymo Research, D4045). Megachunks were then assembled by in vitro ligation overnight at 16°C in 10-μl reaction volumes using 0.1X T4 DNA Ligase (Enzymatics, L6030-HC-L). For ligation, the appropriate gel-

purified chunk fragments were first mixed together and precipitated using ethanol (3 volumes, 100%) and 3 M sodium acetate pH 5.2 (1/10 volume). Instead of equimolar quantities, an ever-decreasing amount of DNA of each chunk in the left to right direction was used to maximize the percentage of correct ligation products containing the selectable marker (e.g., 500 ng E1: 200 ng E2: 100 ng E3).

Two chunks, A1 and B3, were built as partial, nonoverlapping subconstructs that had been sequence-verified. For megachunk A, the two A1 "minichunks" (A1.1 and A1.2) were pre-joined in an equimolar in vitro ligation reaction using a *Pst*I site and gel-purified prior to a second round of in vitro ligation with A2 and A3 (*2*). The DNA corresponding to chunk B3 was delivered in three separate constructs (B3.1, B3.2, B3.3). We designed primers with ~40-bp overhangs to generate overlap between these minichunks as well as a vector sequence [pRS413 (*16*)] capable of single-copy replication in *S. cerevisiae*. The three B3 PCR fragments plus the *Sma*I-linearized pRS413 vector were cotransformed into the WT yeast strain BY4741 for "in yeasto assembly" by homologous recombination. A construct encoding a full-length B3 insert was recovered into *E. coli* from a single yeast colony (pAW006). The insert size was verified by restriction digest and the presence of all synthetic PCRTags confirmed by PCR. However, the sequence of the B3 insert was not verified prior to incorporation into yeast as part of megachunk B. After whole genome sequencing of the synVI yeast strain (yLM093) we discovered seven mutations encoded within the B3 segment (table S2). Subsequent Sanger sequencing of the B3 assembled chunk clone revealed that six of the mutations preexisted in B3 but not in B3.1, B3.2, or B3.3, suggesting they arose during the chunk assembly process, underscoring the importance of sequence-verifying chunks prior to incorporation into yeast.

For megachunk D, an internal *Ava*I site was identified at the junction between the synthetic DNA and the *URA3* selectable marker in chunk D3. This was problematic as *Ava*I had been assigned as the restriction enzyme site for excising chunk D3 at its 5′ end. To overcome this problem, restricted D1, D2, and D3 (missing the *URA3* sequence and 3′ terminal homology to the native chromosome following digestion with *Ava*I) fragments were joined by in vitro ligation and cotransformed into yeast with a PCR-generated *URA3* marker derived from the D3 chunk with ~1-kb terminal homology to the native chromosome.

Integrating megachunks by SwAP-In

SynVI was built from left to right in nine sequential integrative transformations, each involving a "megachunk" of synthetic DNA (A-I) segmented into three or four ~10-kb pieces arbitrarily called "chunks." The rightmost chunk of each megachunk encodes an auxotrophic selectable marker, either *LEU2* or *URA3*. The single exception is megachunk I, which encodes

no marker and was designed to overwrite a pre-existing *URA3* marker in synVI.H. For this reason selection for the full-length synVI chromosome was achieved on 5-FOA (5-fluoro-orotic acid) and yielded an unmarked chromosome. Yeast transformations were carried out using a standard lithium acetate/polyethylene glycol protocol (*17*), except cells were heat shocked for only 15 min in the presence of 10% DMSO at 42°C and prior to plating were incubated in 400 μl 5 mM CaCl₂ for 10 min at room temperature. In all cases the entire in vitro chunk ligation product was transformed into yeast. Strains used for integration (from left to right): yLM097 (*yfl054CΔ::kanMX*), yJS272 (*synVI.A*), yLM067 (*synVI.B*), yLM068 (*synVI.C*), yLM085 (*synVI.D*), yLM086 (*synVI.E*), yLM088 (*synVI.F*), yLM090 (*synVI.G*), yLM091 (*synVI.H*).

Pulsed-field gel electrophoresis

Full-length yeast chromosomes were prepared in agarose plugs as described (*18*). Chromosomes were separated by clamped homogeneous electric field (CHEF) gel electrophoresis using the CHEF-DR III Pulsed-Field Electrophoresis System (Bio-Rad) using the auto algorithm function to separate chromosomes ranging in size from 200 to 500 kb [6 V/cm, switch time 24:03 to 44:69 s, run time 34:02 hours, 14°C, 0.5X Tris-Borate-EDTA buffer, 1% gel prepared with low melting point agarose (Lonza, 50100)]. Gels were stained with 5 μg/ml ethidium bromide in water postelectrophoresis, destained in water, and then imaged.

PCRTag analysis

PCRTag analysis was performed in 2.5-μl reaction volumes using 2X GoTaq Hot Start Colorless Master Mix (Promega, M5132). Master Mix (1X) was arrayed into each well of a 384 well PCR plate (Greiner, 785201) and the acoustic dispenser Echo 550 (LabCyte) was used to transfer genomic DNA [5 nl, prepared as previously described (*19*)] and primers (20 nl, 30 μM premixed forward and reverse) into the appropriate wells. PCR products were analyzed by 1% gel electrophoresis in 1X Tris-Taurine-EDTA or on the LabChip GXII (Perkin-Elmer).

During integration of megachunk D we repeatedly recovered clones that produced both synthetic and WT amplicons at the *YFL009W.2* locus (fig. S2A). We hypothesized the WT PCRTag primers were annealing to a secondary locus in the genome. The WT *YFL009W.2* amplicon sequence was used in a BLAST search against the native yeast genome, returning two hits: its own location on chromosome six, plus a nearly identical region near *YER066W* on chromosome 5 (chrV 289709-290199) (fig. S2B). We deleted the chrV region with a KanMX cassette in the synVI strain to generate yLM096 and repeated the PCRTag analysis. In the absence of the chrV locus the WT *YFL009W.2* PCRTag primers no longer produced an amplicon (fig. S2C).

Genome sequencing

Genomic DNA for sequencing was prepared as described previously (*6*). A whole genome shotgun

library was prepared as follows: 500 ng of genomic DNA were sheared to 500 bp fragments using a Covaris E220 ultrasonicator, and a library was prepared using the Kapa Low-Throughput "With bead" Library Preparation Kit Standard (Kapa Biosystems, KK8231) without any PCR amplification, and sequenced as 50 base paired-end reads on an Illumina HiSeq 2500 (v4 chemistry) machine. Sequence analysis was carried out as previously described (6).

SynVI

The synVI genome sequence was first determined from strain yLM093. Here we discovered a missing loxPsym site in the right arm. Thus, we reintegrated megachunk I into the *synVI.H* strain (yLM091) and verified the sequence across megachunk I using Sanger sequencing in four separate isolates (yLM172 to 175). We discovered 10 variant nucleotides on synVI in the genome of yLM093/yLM175 (table S1). Six of the 10 mutations preexisted in chunk B3, which had been previously assembled from three smaller fragments prior to digestion and in vitro ligation with B1 and B2 for megachunk incorporation. Two alterations occurred at the recoded *Btg*I sticky end junction between chunk D2 and D3, however these sequence variants correspond to the native genome sequence and thus are likely to be a product of "patchwork" homologous recombination (6). The remaining two mutations that give rise to nonsynonymous coding changes are in *RIM15* (*YFL033C*; S1173P) and *MSH4* (*YFL003C*; Y643H) and are presumed to have occurred spontaneously on transformation. The complete genome sequence of the synVI strain encoding corrections to *MOB2* and *PRE4* was also determined (yLM953) at which point we discovered one new variant exclusive to this strain (240434 A to C; *IRC7* T149P) (table S1).

Poly-syn strains

The genome sequence of synIII synVI (yLM890), synIII synIXR (yLM758), synVI synIXR (yLM892), and synIII synVI synIXR (yLM896) were all determined (table S3).

RNA-seq
SynVI

Four isolates of an early version of synVI (yLM172-175; encoding uncorrected versions of *MOB2* and *PRE4*), which correspond to independent transformants from integration of megachunk I, plus a single isolate of a WT strain (BY4741) were used for the initial transcriptome analysis of synVI. In this version of synVI we consistently observed down-regulation of each of the terminal genes synVI genes, *YFL055W* and *YFR055W*, as well as a gene called *HAC1* (*YFL031W*), involved in the unfolded protein response (fig. S5).

A second round of RNA-seq analysis using a "finished" version of synVI (yLM953; encoding corrected versions of *MOB2* and *PRE4*) showed only down-regulation of the terminal genes and *HAC1* expression was unchanged (Fig. 1C). This result was confirmed by qPCR. Down-regulation

of *HAC1* is apparently specific to the early version of synVI through an undetermined mechanism.

Poly-syn strains

The transcriptome of four poly-syn strains (yLM890 synIII synVI; yLM758 synIII synIXR; yLM892 synVI synIXR) was determined by RNA-seq. For this experiment, BY4741 was used as the WT reference strain. BY4741 is a *MAT***a** strain and many of the poly-syn strains are *MAT*α, specifically synIII synVI (yLM890), synIII synIXR (yLM758), synIII synVI synIXR (yLM896) (table S5). Thus, in the RNA-seq data we identified a number of mating type specific genes that were differentially regulated in these three strains (Fig. 3C and fig. S16). Further, we identified expected differential expression of auxotrophic markers (e.g., *MET15*, *LYS2*) in poly-syn strains when the genotype did not match BY4741. The instances of differential expression provide internal controls for our RNA-seq analysis pipeline.

In all poly-syn strains carrying synIII, we observed expression of an allele of *ura3*. This is the result of a mutant *URA3* allele at the *HO* locus, originally used to select for integration of the essential *SYN.SUP61* tRNA. In brief, the essential chromosome III tRNA, *SUP61*, deleted during synIII design (6), was integrated into the *HO* locus on chromosome IV. This integration was achieved with a *URA3* marker (6). While attempting to completely delete the *URA3* selection marker with a spanning PCR product, a frameshift mutation was introduced during selection on FOA rather than deletion of *URA3*, yielding the FOA+, Ura– synIII isolate, yLM422 (6). The error was propagated through all subsequent poly-syn strains carrying synIII. A new set of poly-syn strains correcting this error is available: synIII synVI (yZY455), synIII synIXR (yZY456), synIII synVI synIXR (yZY175) (table S5).

RNA preparation and subsequent analysis of the data for both synVI and the poly-syn RNA-seq experiment was carried out as described (6). For experiments involving yLM953, yLM890, yLM758, yLM892, and yLM896 RNA-Seq library preps were made using the Illumina TruSeq RNA sample Prep Kit v2 (RS-122-2002), using 500 ng of total RNA as input, amplified by 12 cycles of PCR, and run on an Illumina 2500 (v4 chemistry), as paired-end 50.

Preparation of RNA for qPCR analysis

Yeast cultures (5 ml) were grown in YPD overnight at 30°C with rotation. 250 μl of cells were collected by centrifugation at room temperature at 3000 rpm for 3 min. Cells were washed once with water and RNA was extracted using the RNeasy Mini Kit (Qiagen, catalog no. 74106). In brief, RNA was extracted using enzymatic cell lysis with zymolyase and RNA was isolated as per the manufacturer's instructions. DNase treatment was performed on eluted RNA samples (Qiagen, 79254), and the samples were subsequently purified over a second column to remove the DNase. The absence of genomic DNA was verified by qPCR using control gene primers for all samples prior to reverse transcriptase treat-

ment. First strand cDNA was prepared using the SuperScript III First-Strand Synthesis SuperMix (Invitrogen, 18080-400). The expression level of genes of interest was tested using SsoAdvanced SYBR Green Supermix (BioRad, 172-5265) in a 4-μl reaction volume with technical quadruplicates. Here, reactions were assembled using an acoustic droplet ejection robot (Echo 550, LabCyte) to transfer primers (50 nl of 50 μM each premixed; final concentration 0.625 μM each) and cDNA (75 nl) into mastermix pre-arrayed in a 384-well plate (Greiner, 785201). qPCR was performed using the CFX384 Touch Real-Time PCR Detection System (BioRad, 1854-5485) and analysis carried using the CFX Manager Software (BioRad). Single primer pairs targeting each of two reference genes, *UBC6* and *TAF10* (20), were designed.

Generating ρ⁰ strains

Strains were grown for 6 hours in synthetic complete medium or YPD plus 10-μg/ml EtBr and plated for single colonies on YPD. Inability of single colonies to grow on 3% glycerol following replica plating was used to infer the loss of the mitochondrial genome. In some cases the loss of the mitochondrial genome further confirmed by PCR, assessing the presence/absence of amplicons derived from three loci in the mitochondrial genome (*15S rRNA*, *ATP6*, *COX2*).

Correcting two nonsynonymous mutations in MOB2

The essential *MOB2* gene encodes an activator of the Cbk1 kinase and is involved in the RAM (regulation of Ace2 activity and cellular morphogenesis) signaling network regulating cell polarity and morphogenesis (21). We discovered that two nonsynonymous mutations in *MOB2* (T155P and F140L) (table S1), inadvertently introduced during incorporation of megachunk B, resulted in a slow growth defect on 3% glycerol plates at 37°C in the first iteration of the synVI strain (yLM175) (fig. S3A). We mapped the growth defect back to *MOB2* using the following strategy. First, a *MAT***a** ρ⁰ synVI strain (yLM189) derived from yLM175, cured of its mitochondrial genome by growth in ethidium bromide was backcrossed to a *MAT*α WT strain (BY4742) (fig. S3, B and C). Following sporulation of the heterozygous diploid (yLM264), we found the slow growth defect on glycerol at 37°C segregated 2:2 in all tetrads (yLM190-192 and 200-240), suggesting that mutations in the mitochrondrial genome of the synVI strain did not underlie the defect (fig. S3, D to F). Further, using PCRTag analysis we found the defect cosegregated with synthetic PCRTags in all cases (fig. S3, D to F) indicating one or more loci on synVI were likely the cause of the phenotype. We exploited meiotic recombination crossover events between synVI and native VI, tracked via presence or absence of synthetic PCRtags, to map the defect to a 20-kb interval encoding seven genes within chunk B3 (fig. S3, D to G). The B3 synthetic segment encoded four non-synonymous mutations (two each in *MOB2* and *RIM15*) (table S1). Additionally, an

intron in each of *MOB2* and *RPL22B* was deleted during design. Although neither deletion of *RPL22B* (yLM305) nor *RIM15* (yLM548), both nonessential genes, phenocopied the defect in an otherwise WT background, deletion of the essential *WT.MOB2* gene from native chromosome six phenocopied the slow growth defect on glycerol at 37°C in a heterozygous diploid VI/synVI strain (yLM288) (fig. S4A). Consistent with this observation, installing a WT allele of *MOB2* into an otherwise synVI haploid strain rescued the glycerol growth defect (yLM321) (fig. S4B). To test whether the rescue required reintroduction of the *MOB2* intron, repair of the two nonsynonymous mutations, or both, all three alleles were constructed and introduced into the *MOB2* locus on synVI. In haploid cells, we found that correcting the two nonsynonymous mutations (yLM402) was sufficient to restore the fitness of synVI cells growing on glycerol at 37°C back to that observed in the wild type (fig. S4C). Returning the intron in combination with correcting the coding sequence produced no additive effect (yLM366) and returning the *MOB2* intron (yLM383) alone did not rescue the defect (fig. S4C).

MOB2 *strain construction*

SynVI (yLM175) was crossed to BY472 and heterozygous diploids (synVI/VI) selected on medium lacking methionine and lysine (yLM285). *MOB2* was targeted for deletion with a *URA3* cassette by homologous recombination using standard lithium acetate transformation. Eight transformants were tested to determine whether the synthetic (*SYN.MOB2*) or the WT (*WT.MOB2*) allele was deleted based on loss of the amplicon using either the *MOB2* synthetic or WT PCRTag primer pairs (yLM286 *syn.mob2ΔURA3/WT.MOB2*; yLM288 *SYN.MOB2/w*t.mob2ΔURA3). A *MOB2/mob2Δ::URA3* genotype was also constructed in the BY4743 background (yLM290) as well as a synVI/synVI background (yLM294) generated by conditional chromosome destabilization (see below); here deletion of a *MOB2* allele in all strains was validated by standard PCR confirmation. Sporulation and dissection of all heterozygous diploid *MOB2/mob2Δ::URA3* strains tested yielded 2:2 dead:alive spore ratios, where all survivors were Ura-, suggesting that *MOB2* is essential, contrary to some reports (*21*, *22*). WT and synthetic *MOB2* alleles were amplified from BY4741 and synVI (yLM175) genomic DNA (gDNA), respectively, and used to replace the *URA3* cassette in the appropriate heterozygous diploid strains by selecting for transformants resistant to 5-FOA. All integrations were confirmed by PCR.

The *syn.MOB2* allele encoding the repaired nucleotide sequence (*syn.MOB2.2nt*) was PCR amplified from pJS183 using primers encoding 5′ inward-facing *Bsa*I sites and subcloned into the pCR-BluntII-TOPO vector (Invitrogen; cat no 45-0245, Carlsbad, CA) (pLM281). The *syn.MOB2* allele encoding the intron (*syn.MOB2.intron*) was constructed by fusion PCR using one product generated from BY4741 gDNA (promoter, first exon, intron, and 40 bp of the second exon) and

one product generated from the B3 construct (pAW006 with two variant nucleotides; second exon, 3′UTR). Here, the construct was also flanked by inward-facing *Bsa*I sites encoded by the primers, subcloned into pCR-BluntII-TOPO, and sequence-verified (pLM279). The *syn.MOB2* allele encoding both the intron and the repaired nucleotides (*syn.MOB2.intron.2nt*) was constructed and sequence-verified as described for *syn.MOB2.2nt* except pAW006 was used as the template for the part of the construct encoding the second exon (pLM283). In all three cases, *Bsa*I digestion liberated each *syn.MOB2* allele for integration into a *synVI/synVI.syn.mob2Δ::URA3* (yLM294) by homologous recombination. Transformants were selected on 5-FOA and integrations confirmed by PCR. For *syn.MOB2.intron* and *syn.MOB2.intron.2nt*, an intron specific primer was paired with a primer upstream of the integration site. For *syn.MOB2.2nt*, the reverse synthetic *MOB2* PCRTag was paired with a primer whose 3′ terminal nucleotide was either the designed or the mutant nucleotide and PCR conditions optimized for specific amplification (T_m = 62.5°C). Following sporulation and dissection, in all cases the same PCR confirmation primers were used to assess *syn.MOB2* allele segregation.

PCR to test for presence of the mitochondrial genome

The synVI strain (yLM402) was grown to saturation in liquid culture in rich medium (YPD) overnight at 30°C with rotation and plated for single colonies on YPD plates. Following incubation at 30°C for 5 days, the colonies growing on YPD plates were transferred to 3% glycerol plates by replica plating. gDNA from 16 glycerol minus colonies was prepared (*19*), along with gDNA from ρ^+ and ρ^0 WT strain (BY4741 with mitochondrial gDNA intact and BY4741 cured of the mitochondrial gDNA by growth in ethidium bromide). PCR using three primer pairs targeting genes in the mitochondrial genome (*15S RNA*, *ATP6*, *COX2*), plus one primer pair targeting a nuclear gene (*PRE4*) as a positive control was performed and products separated by 1.2% agarose gel electrophoresis in TTE (fig. S6).

RIM15 *and* MSH4

Both *RIM15* and *MSH4* were found to encode nonsynonymous mutations compared to the designed sequence in living synVI strains (yLM175, yLM402, yLM953) (table S1). Each of these two genes were individually deleted with a *URA3* cassette in both the WT (BY4741) and synVI (yLM402) strain backgrounds to generate yLM548, yLM554, yLM545, and yLM551. The deletions were confirmed by PCR. The deletion mutants were used to investigate whether the nonsynonymous mutations were involved in the glycerol-negative growth-suppression defect (fig. S7).

SynVI *and* IXL-synIXR *growth on different media and conditions*

Wild-type (VI and IX, BY4741), synVI (yLM402), and IXL-synIXR (yLM461) strains were grown to saturation in YPD at 30°C with rotation. Cultures

were serially diluted in 10-fold increments in water and plated onto each type of medium (fig. S8). All drugs [methane methanesulfate (MMS) (Sigma, 129925), Benomyl (Aldrich, 381586), camptothecin (Sigma, C9911), hydroxyurea (HU) (Sigma, H8627)] were mixed into rich medium (YPD) except 6-azauracil (Sigma, A1757), which was mixed in synthetic complete medium containing dextrose. YPGE was prepared with 2% glycerol and 2% ethanol. High- and low-pH plates (9.0 and 4.0) were prepared using NaOH and HCl respectively in YPD. Sorbitol plates were prepared by adding the appropriate quantity of sorbitol (Sigma, S1876). For hydrogen peroxide (Fluka, 88597) and cycloheximide (Sigma C7698), overnight cultures were treated for 2 hours in drug, harvested by centrifugation and resuspended in water prior to plating the serial dilutions on YPD. Plates were incubated at 30°C unless otherwise indicated in fig. S8 for 2 days (YPD, camptothecin, 6-azauracil, Benomyl, pH4.0, pH9.0, cycloheximide, hydrogen peroxide) or 3 days (sorbitol, YPGE, HU, MMS).

SynVI backcross to map glycerol-negative growth-suppression defect to megachunk H

The synVI strain with a corrected *MOB2* allele (yLM402) displayed the glycerol-negative growth-suppression defect. To map the defect, two spontaneously generated synVI (yLM402) glycerol-negative colonies were mated to BY4742 and diploids selected on synthetic medium lacking lysine and methionine (yLM578 and yLM579). Following sporulation and dissection, eight tetrads derived from each parent strain (yLM578 = tetrads 1 to 8; yLM579 = tetrads 9 to 16 in fig. S9) were subjected to PCRTag analysis using fifteen synthetic PCRTags spaced evenly along the length of the chromosome and further assessed which of the 64 spores had inherited the glycerol-negative growth-suppression defect (Fig. 1F and fig. S9). In all cases the defect segregated 2:2 with the right arm of synVI. The entire set of 164 synthetic PCRTag amplicons was then used to test two spores, 10B and 13A, for their synthetic DNA content (fig. S10A). As a result, the defect was mapped to a ~30-kb region encompassing megachunk H (YFR034C to YFR053C) (fig. S10B).

tK(CUU)F *and* YFR045W *intron*

Two genes in the glycerol-negative growth-suppression defect mapped interval had annotations relevant to mitochondrial function: deletion of a tRNA [*tK(CUU)F*] that is imported into the mitochondria (*23*), and deletion of the intron in *YFR045W*, encoding a putative mitochondrial import protein. *tK(CUU)F* was targeted for deletion with a *URA3* cassette by homologous recombination in BY4741 using standard homologous recombination techniques to generate *tK(CUU)FΔ::URA3* (yLM748). Similarly, *YFR045W* was targeted for deletion with a *URA3* cassette by homologous recombination in both BY4741 and synVI (yLM402) using standard homologous recombination techniques to generate *yfr045wΔ::URA3* (yLM698 and yLM699, respectively).

The *WT.YFR045W* and *SYN.YFR045W* alleles were amplified from the appropriate gDNA (BY4741 or yLM402, respectively) and the resulting PCR products transformed into the appropriate *yfr045w∆:: URA3* strains (*WT.YFR045W* into yLM699 and *SYN.YFR045W* into yLM698) and selection achieved on 5-FOA. Integrations were confirmed by PCR. Neither deletion of the tRNA nor intron in a WT background provoked a glycerol-negative growth-suppression defect (fig. S11).

Circularization of synVI and native VI

The *URA3* gene was amplified with primers encoding ~40-bp overhangs targeting the two ends of synVI, just inside the core X elements, for homologous recombination to generate a ring chromosome VI structure (native VI or synVI) (fig. S12A). A version of the *URA3* gene that could enable downstream linearization via the telomerator was used (*24*). Strains with the resultant native VI and synVI ring chromosomes were identified by PCR with primers spanning the *URA3* gene and the absence of the native VI or synVI band tested by pulsed-field gel (ring chromosomes do not penetrate pulsed-field gels) (Fig. 1B and fig. S12B; yLM717 and yLM728). Of the recovered ring synVI transformants, a single isolate lacked the glycerol-negative growth-suppression defect, whereby the colony size and morphology matched that of native VI strains (circular or linear) (fig. S12C). Pulsed-field gel analysis revealed a structural rearrangement within the synVI chromosome in this strain resulting in a linear chromosome ~360 kb long. Genome sequencing of the "triplication strain" (yLM644) revealed the rightmost 60 kb of the synthetic chromosome was present in three copies based on sequence read depth (fig. S12D). That triplication of the right arm of synVI rescues the glycerol-negative growth-suppression defect suggests that increased copy number of one or more genes contained in this segment underlies the defect.

Converting synVI chunks to evaluate glycerol-negative growth-suppression defect complementation in yeast

The glycerol-negative growth-suppression defect mapped to a ~30-kb interval on the right arm of synVI encoding 23 genes, encompassing *YFR034C* to *YFR053C*, spanning chunks H2, H3, and H4. To investigate whether increased copy number of any DNA in these chunks could rescue the glycerol-negative growth-suppression defect, we converted each chunk construct for replication and segregation in yeast by introducing a centromere (CEN), autonomously replicating sequence (ARS), and selectable marker (*HIS3*) (fig. S13).

A distinct restriction site flanking the synVI chunk insert was identified and used to linearize each of H2 (pLM173, *Blp*I), H3 (pLM174, *Not*I) and H4 (pLM175, *Bam*HI) chunks. Following agarose gel electrophoresis (0.8%), linearized chunks were gel-purified. Primers were designed to anneal on either side of the CEN/ARS/*HIS3* segment of pRS413 (*16*), and additionally encode ~40 bp of overhang sequence to the terminal ends of the linearized chunk sequences. Following PCR, the

CEN/ARS/*HIS3* fragments were gel-purified. The corresponding linearized chunk and CEN/ARS/*HIS3* fragments were cotransformed into yeast for assembly by homologous recombination and selection carried out on synthetic medium lacking histidine (SC–His). For each of the three assemblies, yeast transformants were pooled and plasmids recovered into *E. coli* (Top10 cells) as previously described except the blue-white screening step was omitted (*25*). A correctly assembled clone was identified by analyzing the restriction digestion pattern using three sepate enzymes (*Afl*II, *Bsi*WI, and *Xcm*I) and subsequently transformed into both synVI and WT yeast cells in addition to an empty vector. The H2, H3, and H4 chunk constructs converted for expression in yeast are stored as pLM356, pLM357, and pLM370, respectively.

To evaluate complementation, three independent transformants were inoculated into SC–His liquid medium and incubated with rotation overnight at 30°C. Single colonies from each strain were then plated on SC–His plates and incubated for 4 days at 30°C. The growth defect was measured as a percent of the petite colonies compared to the total number of colonies growing (fig. S13). We observed that the petite frequency was much less prominent in the synVI strain on SC–His medium (~15% rather than ~50% on rich medium). When expressed in the synVI strain only chunk H3 rescued the defect (Fig. 2E).

Cloning YFR047C, YFR048W, YFR049W, YFR050C, YFR051C, and YFR052W

Each synthetic gene encoded within H3 was subsequently cloned individually for expression in yeast. Primers that annealed ~500 bp upstream of the start codon and ~200 bp downstream of the stop codon were designed with ~40-bp overhang sequence homologous to the terminal ends of a *Bsa*I-digested custom CEN/ARS shuttle vector marked with KanMX (pLM200). Each gene was amplified from synVI yeast genomic DNA and assembled into the linearized pLM200 vector by one-step isothermal assembly (*26*) and transformed into *E. coli* (Top10). Clones encoding the correctly sized insert were identified by restriction digestion from plasmid DNA prepared from overnight cultures grown in LB supplemented with carbenicillin (75 µg/ml). [*YFR047C*], [*YFR048W*], [*YFR049W*], [*YFR050C*], [*YFR051C*], and [*YFR052W*] are stored as pLM364, pLM365, pLM367, pLM368, pLM370, and pLM385, respectively. We found that increased copy number of *YFR050C*, encoding *PRE4*, could rescue the defect (fig. S13).

PRE4 strain construction

PRE4 is an essential gene. A synVI homozygous diploid strain was generated by mating a ρ⁰ synVI cell (yLM450) to a WT chromosome VI strain encoding the *pGAL1-CEN6::URA3(Kl)* contruct (yLM245) (*27*) in place of the native chromosome VI centromere (yLM661). Diploids were selected by streak purifying on SC medium lacking methionine, uracil, and lysine. A single colony was inoculated into yeast extract/peptone/galactose (YP galactose) liquid medium and

incubated at 30°C with rotation for 18 hours. 200 µl of culture was spread evenly onto a plate with synthetic complete medium supplemented with 5-FOA and extra uracil and after incubation at 30°C for 2 days, eight single colonies were streak purified on the same type of medium. The presence of synthetic DNA and absence of WT DNA was assessed by PCRtagging with ~15 synthetic and WT PCRtags, evenly spaced along the length of chromosome six. A single clone was subsequently tested using the entire panel of synthetic and WT PCRtags to verify loss of the full-length WT chromosome (i.e., 2N-1). To determine whether the synVI chromosome had endoreduplicated, four single colonies derived from the 2N-1 strain were subjected to sporulation and tetrad dissection. In all four cases the growth of almost entirely four spore tetrads was consistent with endoreduplication. The homozygous diploid synVI strain was named yLM544. One copy of *PRE4* was targeted for deletion with a *URA3* cassette by homologous recombination using standard lithium acetate transformation in the WT VI/VI (BY4743) and synVI/synVI (yLM544) diploid strains and the deletion confirmed by PCR (yLM770 and yLM772, respectively). A plasmid encoding WT *PRE4* ([*WT.PRE*], pLM394 as described above) was transformed into yLM770 and yLM772 and both strains were subjected to sporulation and tetrad dissection. Spores that were Ura⁺, G418ʳ and had also inherited the classic *MATa* and *MATα* genotype configurations associated with "Boeke Yeast" (BY) strains BY4741 and BY4742 (*28*) (*MATa LYS2 met15∆; MATα lys2∆ MET15*) were selected (*synVI pre4∆::URA3 [WT.PRE4] yLM823; VI pre4∆::URA3 [WT.PRE4] yLM819*). Alleles of *PRE4*, constructed as described below, were integrated directly into the *pre4∆::URA3* locus by selection on 5-FOA in one of two ways: (i) DNA was transformed into the heterozygous diploid strains (yLM770 and yLM772) and following sporulation and dissection, spores carrying the *PRE4* allele of interest were identified by PCR; or (ii) DNA was transformed into the haploid *pre4∆* strains expressing *PRE4* episomally (yLM819 and yLM823) and following selection on 5-FOA the loss of the *WT.PRE4* plasmid confirmed by replica plating and identifying G418 sensitive colonies. In all cases, the correct integration was identified by PCR. Thus for all strains generated to study the relationship between *PRE4* and the glycerol-negative growth-suppression defect, *PRE4* was integrated into the precise chromosomal location and expressed under the control of the *PRE4* promoter, including the N-terminally tagged *HA-PRE4* strains.

After integration of *SYN.PRE4*, *WT.PRE4*, *SYN-WT.PRE4*, and *WT-SYN.PRE4* alleles into yLM823, each strain was "cured" of its mitochondrial genomic DNA by growth in ethidium bromide (describe above). A ρ⁰ isolate was then crossed to a native VI *pGAL-CEN6* strain (yLM661) and the native chromosome VI destabilized in the resulting diploid strain by growth in galactose (described below). Following sporulation and dissection haploid strains with "clean" mitochondrial gDNA populations were isolated (synVI *SYN.PRE4*, yLM945; synVI *WT.PRE4*,

yLM949; synVI SYN-WT.PRE4, yLM953; synVI WT-SYN.PRE4, yLM957). Following this "endor-eduplication backcross" to introduce WT populations of mitochondria, the glycerol-negative growth-suppression defect was not cured in the strains encoding the SYN.PRE4 allele.

Constructing PRE4 alleles

WT.PRE4 and SYN.PRE4 alleles were generated by PCR using genomic DNA extracted from WT (BY4741) and synVI (yLM402) cells as template, respectively. The primers annealed ~500 bp upstream and ~200 bp downstream of the PRE4 start and stop codons to provide template for homologous recombination upon transformation into yeast cells. The PCR products were transformed into heterozygous diploid PRE4/preΔ strains encoding two copies of native chromosome VI (yLM770) or two copies of synVI (yLM772) with selection on 5-FOA. After confirming integration by PCR, the strains were subjected to sporulation and dissection to generate WT haploid cells carrying the synthetic PRE4 allele (VI SYN.PRE4, yLM849) or synVI cells carrying the WT PRE4 allele (synVI WT.PRE4, yLM848). Segregation of the synthetic and WT alleles in spores was tested by PCRTag primers and in all cases segregated two to two.

WT-SYN.PRE4 and SYN-WT.PRE4 alleles were constructed by separately amplifying the 5′ and 3′ halves of each of SYN.PRE4 and WT.PRE4, splitting the gene between the two PCRTags. The PCR amplicons encoded 40-bp terminal sequence homology to facilitate fusion PCR to generate WT-SYN.PRE4 and SYN-WT.PRE4 alleles by pairing the appropriate PCR products. Fusion PCR amplicons were subcloned into the pCR-BluntII-TOPO vector (Invitrogen; 45-0245) and sequence-verified (pLM433 WT-SYN.PRE4; pLM435 SYN-WT.PRE4). For integration into yLM823 and yLM819 the alleles were excised from the plasmid backbones by double digestion with BsaI and SspI.

N-terminally tagged 3HA PRE4 alleles were generated by fusion PCR of three separate amplicons: (i) ~300 bp upstream of the PRE4 ATG, (ii) 3HA tag, which was ordered as an ultramer from Integrated DNA Technologies (IDT), and (iii) the PRE4 coding sequence plus ~200 bp downstream of the stop codon. The fusion PCR product was subcloned into the pCR-BluntII-TOPO vector (Invitrogen; 45-0245) and sequence-verified (HA-WT.PRE4 pLM437; HA-SYN.PRE4 pLM432). For integration into yLM823 and yLM819 the alleles were excised from the plasmid backbones by double digestion with BsaI and SspI.

To construct PRE4 alleles in which individual synthetic codons were replaced with the WT versions (across the 3′ PCRTag), PCR products were generated corresponding to the 5′ and 3′ halves of PRE4, splitting the gene within the 3′ PCRTag and encoding the WT codon in the overlapping primer. Fusion PCR products, generated with the flanking primer pairs, were used directly for yeast transformation (codon 1, yLM1004; codon 2, yLM1006; codon 3, yLM1008; codon 4, yLM1010; codon 5, yLM1012; codon 6, yLM1014; codon 7, yLM1016; codon 8, yLM1018; codon 9,

yLM1020; codon 10, yLM1022). Integrations were confirmed by PCR and single codon changes validated by sequencing.

The SYN.PRE4.WT.RSSR and WT.PRE4.SYN.RSSR alleles were also generated by fusion PCR, whereby the four codons to be changed were encoded within overlapping central primers. The 5′ and 3′ PCR products were subjected to fusion PCR with the two flanking primers and products were subcloned into the pCR-BluntII-TOPO vector (Invitrogen; 45-0245) and sequence-verified (SYN. PRE4.WT.RSSR, pLM444; WT.PRE4.SYN.RSSR, pLM445). For integration into yLM823 and yLM819 the alleles were excised from the plasmid backbones by double digestion with BsaI and SspI.

SynIII synVI synIXR proteome analysis
Cell growth

BY4741 and synIII synVI synIXR cultures (200 ml), transformed with a plasmid encoding a kanMX cassette (pLM200), were grown in YPD + G418 at 30°C to an OD of 1.0. Cell pellets were collected by centrifugation (3000 rpm, 3 min) at 4°C and washed once with ice cold water and subsequently frozen at –80°C.

Cell lysis

Cells were lysed in 15-ml centrifuge tubes in TMT lysis buffer [10 mM Tris/HCl (pH 8.0), 8 M urea, 0.15% deoxycholate] plus protease inhibitor (Roche, 11873580001, added just prior to lysis) and 0.5-mm glass beads (10:1 ratio of lysis buffer to cells, 2:1 volume of cell slurry to beads). Lysis was achieved in 10 × 30 s vortex blasts separated by 1 min of rest on ice followed by 3 × 20 s sonication steps (Sonicator Xx, setting 4). Sonication was performed at 4°C with 2 min of recovery time between pulses.

Protein digestion

Lysate protein concentration was measured at 280 nm using a NanoDrop DS-11 Spectrophotometer (DeNovix). Disulfide bonds were reduced by addition of 5 mM dithiothreitol (DTT) and incubated for 1 hour at 55°C. The mixture was cooled to room temperature, and the reduced cysteine residues were alkylated by addition of 14 mM iodoacetamide and incubation in the dark at room temperature for 45 min. Excess iodoacetamide was quenched with an additional 5 mM dithiothreitol. The cell lysate was digested with Lys-C (Promega, 200:1 by weight) at room temperature for 2 hours in lysis buffer (8 M urea, 10 mM Tris-HCl, pH 8.5), then the urea concentration was diluted to 2 M by addition of 10 mM Tris-HCl, pH 8.5 and the sample digested with Trypsin (Promega, 100:1 by weight) at room temperature overnight. The sample was acidified with TFA to pH < 3 and desalted using C18 solid-phase extraction (SPE, Sep-Pak, Waters), and eluted with 80% acetonitrile (ACN) in 0.5% acetic acid. The eluent was dried in the Speedvac and stored at –80°C until further analysis.

TMT labeling

The desalted peptides were re-suspended in 70 μl of 50 mM HEPES (pH 8.5). Approximately

180 μg of peptides from each sample were labeled with TMT reagent according to manufacturer's protocol (Thermo Scientific, 90110). 20 μg of peptides from each of the 9 individual samples were combined and used as a universal standard. The TMT reagents (0.8 mg) (Thermo Scientific) were dissolved in 44 μl of ACN, 10 μl was added to each sample along with 20 μl of ACN. After incubating for 1 hour at room temperature (25°C), the reaction was quenched with 4 μl of 5% w/v hydroxylamine. Following labeling, the samples were combined in equal ratio. The pooled sample was desalted over SCX and SAX solid-phase extraction columns (SPE, STRATA, Phenomenex).

Offline basic-pH RP fractionation

The pooled TMT labeled sample was subjected to basic-pH reverse-phase HPLC for fractionation. The mixture was solubilized in buffer A (10 mM ammonium formate, pH 10.0). Basic pH HPLC was performed on a 4.6 mm × 250 mm Xbridge C18 column (Waters, 3.5 μm bead size) using an Agilent 1260 HPLC instrument. A 30-min linear gradient from 10 to 50% solvent B (90% ACN, 10 mM ammonium formate, pH 10.0) at a flow rate of 0.5 ml/min separated the peptide mixture into a total of 30 fractions. The 30 fractions were pooled into 10 final fractions by combining early, middle, and late eluting RPLC fractions. The concatenated samples were then dried in the Speedvac and stored at –80°C till LC-MS/MS analysis.

LC-MS/MS

Concatenated samples were analyzed with the Q-Exactive mass spectrometer (Thermo Scientific) coupled to an EASY-nLC (Thermo Scientific) liquid chromatography system. The sample was first loaded onto a trap column (Acclaim PepMap 100 pre-column, 75 μm × 2 cm, C18, 3 μm, 100 Å, Thermo Scientific) and then separated on an analytical column (EASY-Spray column, 50 cm × 75 μm ID, PepMap RSLC C18, 2 μm, 100 Å, Thermo Scientific) maintained at a constant temperature (45°C) and equilibrated with 5% buffer A (2% acetonitrile, 0.5% acetic acid). Peptides were separated with a 120-min linear gradient of 5 to 30% buffer B (90% acetonitrile, 0.5% acetic acid) at a flow rate of 200 nl/min. Each full MS scan [Resolution (R) = 70,000 @ m/z 200] was followed by data dependent MS2 scan (R = 35,000 @ m/z 200) with HCD and an isolation window of 1.6 m/z. Normalized collision energy was set to 27, target value of 1e6 for MS1 and 5 × 10^4 for MS2, maximum ion time 50 and 180 ms for MS1 and MS2, respectively, monoisotopic precursor selection was enabled and the dynamic exclusion was set to 15.0 s.

Data analysis

Raw mass spectrometry data were processed using MaxQuant version 1.5.2.8, with a false-discovery rate (FDR) of 0.01 at the level of proteins and peptides, using the following settings: oxidized methionine (M), acetylation (protein N-term) and deamidation (NQ) were selected as variable modifications, and carbamidomethyl

(C) as fixed modifications; precursor mass tolerance 10 ppm; fragment mass tolerance 0.01 Th; and minimum peptide length of six amino acids. Proteins and peptides were identified using a target-decoy approach with a reversed database, using the Andromeda search engine integrated into the MaxQuant environment. Searches were performed against the UniProt *S. cerevisiae* FASTA database. The following filters and criteria were used for quantification: (i) Only distinctive peptides were used for quantification, and only proteins with at least 2 distinctive peptides were quantified. (ii) The minimum reporter ion intensity was set to 1000. Bioinformatics analysis was performed with Perseus, Microsoft Excel and R statistical computing software. Each reporter ion channel was summed across all quantified proteins and normalized assuming equal protein loading across all ten samples. Welch's *t* test was then used to identify proteins that were differentially expressed across each sample triplicates, and the method of permutation-based FDR (*29*) was subsequently applied to control for multiple testing error.

Direct testing of protein levels in synIII synVI synIXR

From the list of eleven proteins with altered expression level detected in the TMT proteome analysis of synIII synVI synIXR, six were selected for direct testing by Western blot analysis. His2 was chosen because it is encoded by synVI. Sac7, Snu114, Has1, and Chs2 were chosen because they are encoded by essential genes. Cox5A was chosen because it is an inner mitochondrial membrane protein. Each gene was C-terminally tagged with a 3-HA tag using *HIS3* selection as previously described (*30*) in both WT cells (BY4742) and the synIII synVI synIXR strain (yLM896). All strains were confirmed by PCR (yLM1104-yLM1127). Two independent transformants from each of the WT and triple-syn strain backgrounds were used to assess protein level by immunoblot (fig. S17).

HIS2-HA (native HIS2 3′ sequence) strain construction in synVI

HIS2 was deleted with a *URA3* cassette in a WT (BY4741) and synVI (yLM953) strain background to generate yLM1130 and yLM1131, respectively. The deletions were confirmed by PCR. Synthetic and WT C-terminally tagged *HIS2-HA* alleles were generated by fusion PCR of three parts: (i) 200 bp upstream of the start codon to the last coding amino acid, excluding the stop codon; (ii) 3xHA sequence amplified from a preexisting plasmid (*30*); and (iii) ~200 bp downstream of the stop codon, excluding the loxPsym site from the synthetic *HIS2* allele. Synthetic or WT *HIS2* sequences were amplified from synVI (yLM953) or WT (BY741) genomic DNA, respectively. Primers for the three segments were designed to yield 20 to 30 bp of terminal homology between adjacent parts to facilitate fusion PCR. Further, the right- and leftmost primers encoded inward facing *Bsa*I site to excise the fragment from a vector in subsequent steps. Fusion PCR products were subcloned into the pCR-BluntII-TOPO vec-

tor (Invitrogen; 45-0245) and sequence-verified (*SYN.HIS2-HA*, pLM532; *WT.HIS2-HA*, pLM533). For integration into yLM1130 and yLM1131 the alleles were excised from the plasmid backbones by digestion with *Bsa*I. The digestion product was transformed and following selection on 5-FOA, transformants confirmed by PCR (chrVI *WT.HIS2-HA*, yLM1147; chrVI *SYN.HIS2-HA*, yLM1150, synVI *WT.HIS2-HA*, yLM1153; synVI *SYN.HIS2-HA*, yLM1156). To modify the region 5′ of *HIS2*, encoding either a tRNA gene (tA(AGC)F) in the WT strain or a loxPsym site in the synVI strain, a *URA3* cassette targeting deletion of these features was transformed into yLM1147, yLM1150, yLM1153, and yLM1156 and confirmed by PCR in all cases. PCR products spanning the tRNA or the loxPsym site (200 bp of flanking homology) derived from WT (BY4741) or synVI (yLM953) cells were then used to overwrite the *URA3* sequence by selection on 5-FOA (chrVI *loxPsym WT.HIS2-HA*, yLM1199; chrVI *loxPsym SYN.HIS2-HA*, yLM1201; synVI *tRNA WT.HIS2-HA*, yLM1203; synVI *tRNA SYN.HIS2-HA*, yLM1205).

Immunoblot analysis

For both HA-Pre4, evaluation of TMT proteome results, and His2-HA experiments, cells were grown to mid-log phase at 30°C in YPD medium, collected by centrifugation, washed once in ice cold water, and immediately frozen at –80°C. Cells were lysed in an equal volume of lysis buffer [20 mM HEPES, pH 7.4, 0.1% Tween 20, 2 mM MgCl$_2$, 300 mM NaCl, protease inhibitor cocktail (Roche, 11873580001)] in the presence of 0.5 mm glass beads (1:1 cell slurry:beads) by vortexing (7 × 1 min blasts with 1-min incubation on ice between each blast). Following centrifugation (14000 rpm, 4°C, 10 min), 30 μl of clarified whole-cell extract was mixed with 10 μl 4X LDS sample buffer (premixed with beta mercaptoethanol) (Life Technologies, NP0007). Samples were heated at 70°C for 10 min and loaded onto a 4 to 12% pre-cast Bis-Tris gel (Life Technologies, NP03222) and electrophoresed in 1x MES buffer. Protein transfer was carried out using a BioRad Trans-blot Turbo Transfer system and corresponding reagents. Anti-HA antibody was from Covance (MMS-101P; mouse) and Anti-Tub1 (Rabbit) served as a control for loading. Secondary antibodies were from LI-COR (IRDye 800CW, 926-32210; IRDye 680RD, 926-68071). Western blots were developed and quantified using the LI-COR Odyssey and Image Studio Software.

Strains and media

The list of "final" synthetic strains used in this study is listed in table S5. SynVI strain versions are listed in table S6, including details on mutations identified on synVI in each strain. All media and growth conditions were standard. 3% glycerol plates were prepared with 3% glycerol (v/v) as the sole carbon source, omitting dextrose entirely from the recipe.

REFERENCES AND NOTES

1. S. Richardson et al., Design of a synthetic yeast genome. Science **355**, 1040–1044 (2017).

2. J. S. Dymond et al., Synthetic chromosome arms function in yeast and generate phenotypic diversity by design. Nature **477**, 471–476 (2011). doi: 10.1038/nature10403; pmid: 21918511

3. R. E. Chapman, P. Walter, Translational attenuation mediated by an mRNA intron. Curr. Biol. **7**, 850–859 (1997). doi: 10.1016/S0960-9822(06)00373-3; pmid: 9382810

4. U. Rüegsegger, J. H. Leber, P. Walter, Block of HAC1 mRNA translation by long-range base pairing is released by cytoplasmic splicing upon induction of the unfolded protein response. Cell **107**, 103–114 (2001). doi: 10.1016/S0092-8674(01)00505-0; pmid: 11595189

5. See Materials and methods section.

6. N. Annaluru et al., Total synthesis of a functional designer eukaryotic chromosome. Science **344**, 55–58 (2014). doi: 10.1126/science.1249252; pmid: 24674868

7. J. L. Schreve, J. M. Garrett, Yeast Agp2p and Agp3p function as amino acid permeases in poor nutrient conditions. Biochem. Biophys. Res. Commun. **313**, 745–751 (2004). doi: 10.1016/j.bbrc.2003.11.172; pmid: 14697254

8. M. Roncoroni et al., The yeast IRC7 gene encodes a β-lyase responsible for production of the varietal thiol 4-mercapto-4-methylpentan-2-one in wine. Food Microbiol. **28**, 926–935 (2011). doi: 10.1016/j.fm.2011.01.002; pmid: 21569935

9. G. Fourel, E. Revardel, C. E. Koering, E. Gilson, Cohabitation of insulators and silencing elements in yeast subtelomeric regions. EMBO J. **18**, 2522–2537 (1999). doi: 10.1093/emboj/18.9.2522; pmid: 10228166

10. W. Hilt, C. Enenkel, A. Gruhler, T. Singer, D. H. Wolf, The PRE4 gene codes for a subunit of the yeast proteasome necessary for peptidylglutamyl-peptide-hydrolyzing activity. Mutations link the proteasome to stress- and ubiquitin-dependent proteolysis. J. Biol. Chem. **268**, 3479–3486 (1993). pmid: 8381431

11. P. C. Ramos, A. J. Marques, M. K. London, R. J. Dohmen, Role of C-terminal extensions of subunits β2 and β7 in assembly and activity of eukaryotic proteasomes. J. Biol. Chem. **279**, 14323–14330 (2004). doi: 10.1074/jbc.M308757200; pmid: 14722099

12. M. Groll et al., Structure of 20S proteasome from yeast at 2.4 Å resolution. Nature **386**, 463–471 (1997). doi: 10.1038/386463a0; pmid: 9087403

13. W. Heinemeyer, M. Fischer, T. Krimmer, U. Stachon, D. H. Wolf, The active sites of the eukaryotic 20 S proteasome and their involvement in subunit precursor processing. J. Biol. Chem. **272**, 25200–25209 (1997). doi: 10.1074/jbc.272.40.25200; pmid: 9312134

14. K. M. Chan, Y. T. Liu, C. H. Ma, M. Jayaram, S. Sau, The 2 micron plasmid of Saccharomyces cerevisiae: A miniaturized selfish genome with optimized functional competence. Plasmid **70**, 2–17 (2013). doi: 10.1016/j.plasmid.2013.03.001; pmid: 23541845

15. Y. Wu et al., Bug mapping and fitness testing of chemically synthesized chromosome X. Science **355**, eaaf4706 (2017).

16. R. S. Sikorski, P. Hieter, A system of shuttle vectors and yeast host strains designed for efficient manipulation of DNA in Saccharomyces cerevisiae. Genetics **122**, 19–27 (1989). pmid: 2659436

17. R. D. Gietz, Yeast transformation by the LiAc/SS carrier DNA/PEG method. Methods Mol. Biol. **1205**, 1–12 (2014). doi: 10.1007/978-1-4939-1363-3_1; pmid: 25213235

18. M. Lisby, U. H. Mortensen, R. Rothstein, Colocalization of multiple DNA double-strand breaks at a single Rad52 repair centre. Nat. Cell Biol. **5**, 572–577 (2003). doi: 10.1038/ncb997; pmid: 12766777

19. J. S. Dymond, Preparation of genomic DNA from Saccharomyces cerevisiae. Methods Enzymol. **529**, 153–160 (2013). doi: 10.1016/B978-0-12-418687-3.00012-4; pmid: 24011043

20. M. A. Teste, M. Duquenne, J. M. François, J. L. Parrou, Validation of reference genes for quantitative expression analysis by real-time RT-PCR in Saccharomyces cerevisiae. BMC Mol. Biol. **10**, 99 (2009). doi: 10.1186/1471-2199-10-99; pmid: 19874630

21. E. L. Weiss et al., The Saccharomyces cerevisiae Mob2p-Cbk1p kinase complex promotes polarized growth and acts with the mitotic exit network to facilitate daughter cell-specific localization of Ace2p transcription factor. J. Cell Biol. **158**, 885–900 (2002). doi: 10.1083/jcb.200203094; pmid: 12196508

22. L. Schneper, A. Krauss, R. Miyamoto, S. Fang, J. R. Broach, The Ras/protein kinase A pathway acts in parallel with the Mob2/Cbk1 pathway to effect cell cycle progression and proper bud site selection. Eukaryot. Cell **3**, 108–120 (2004). doi: 10.1128/EC.3.1.108-120.2004; pmid: 14871942

23. R. P. Martin, J. M. Schneller, A. J. Stahl, G. Dirheimer, Import of nuclear deoxyribonucleic acid coded lysine-accepting transfer ribonucleic acid (anticodon C-U-U) into yeast mitochondria. *Biochemistry* **18**, 4600–4605 (1979). doi: 10.1021/bi00588a021; pmid: 387075

24. L. A. Mitchell, J. D. Boeke, Circular permutation of a synthetic eukaryotic chromosome with the telomerator. *Proc. Natl. Acad. Sci. U.S.A.* **111**, 17003–17010 (2014). doi: 10.1073/pnas.1414399111; pmid: 25378705

25. Q. Lin *et al.*, RADOM, an efficient in vivo method for assembling designed DNA fragments up to 10 kb long in *Saccharomyces cerevisiae*. *ACS Synth. Biol.* **4**, 213–220 (2015). pmid: 24895839

26. D. G. Gibson *et al.*, Enzymatic assembly of DNA molecules up to several hundred kilobases. *Nat. Methods* **6**, 343–345 (2009). doi: 10.1038/nmeth.1318; pmid: 19363495

27. R. J. Reid *et al.*, Chromosome-scale genetic mapping using a set of 16 conditionally stable *Saccharomyces cerevisiae* chromosomes. *Genetics* **180**, 1799–1808 (2008). doi: 10.1534/genetics.108.087999; pmid: 18832360

28. C. B. Brachmann *et al.*, Designer deletion strains derived from *Saccharomyces cerevisiae* S288C: A useful set of strains and plasmids for PCR-mediated gene disruption and other applications. *Yeast* **14**, 115–132 (1998). doi: 10.1002/(SICI)1097-0061(19980130)14:2<115::AID-YEA204>3.0.CO;2-2; pmid: 9483801

29. S. J. Humphrey, S. B. Azimifar, M. Mann, High-throughput phosphoproteomics reveals in vivo insulin signaling dynamics. *Nat. Biotechnol.* **33**, 990–995 (2015). doi: 10.1038/nbt.3327; pmid: 26280412

30. M. S. Longtine *et al.*, Additional modules for versatile and economical PCR-based gene deletion and modification in *Saccharomyces cerevisiae*. *Yeast* **14**, 953–961 (1998). doi: 10.1002/(SICI)1097-0061(199807)14:10<953::AID-YEA293>3.0.CO;2-U; pmid: 9717241

31. M. Zuker, Mfold web server for nucleic acid folding and hybridization prediction. *Nucleic Acids Res.* **31**, 3406–3415 (2003). doi: 10.1093/nar/gkg595; pmid: 12824337

Editor's Summary

Article Tools	Visit the online version of this article to access the personalization and article tools: http://science.sciencemag.org/content/355/6329/eaaf4831
Permissions	Obtain information about reproducing this article: http://www.sciencemag.org/about/permissions.dtl